Construction of a CRISPR-Biolayer Interferometry Platform for Real-Time, Sensitive, and Specific DNA Detection

Shan-Peng Qiao,[a] Zhen-Ni Liu,[a] Hai-Chao Li,[a] Xin He,[b] Hong Pan,[a] and Yu-Zhou Gao*[a, c]

The clustered regularly interspaced short palindromic repeats (CRISPR) technology has been widely applied for nucleic acid detection because of its high specificity. By using the highly specific and irreversible bond between HaloTag and its alkane chlorine ligand, we modified dCas9 (deactivated CRISPR/Cas9) with biotin as a biosensor to detect nucleic acids. The CRISPR biosensor was facilely prepared to adequately maintain its DNA-recognition capability. Furthermore, by coupling biolayer interferometry (BLI) with the CRISPR biosensor, a real-time, sensitive, and rapid digital system called CRISPR-BLI was established for the detection of double-stranded DNA. The CRISPR biosensor immobilised on the biolayer could recruit the target DNA onto the biosensor surface and change its optical thickness, resulting in a shift in the interference pattern and responding signal of the BLI. The CRISPR-BLI system was further applied to detect the *ALP* gene of *Escherichia coli* DH5α combined with a polymerase chain reaction, which demonstrated a linear range from 20 to 20000 pg and a low detection limit (1.34 pg). The CRISPR-BLI system is a promising approach for rapid and sensitive detection of target DNA analytes.

Introduction

Advances in genome sequencing approaches have facilitated the recognition of various target sequence biomarkers involved in several pathologies.[1–3] These advances have led to the development of specific nucleic acid detection methods and molecular diagnostic assays.[4–6] Molecular diagnostics is a powerful tool applied in various fields, such as diseases, food safety, and environmental monitoring,[7–10] Some of these approaches play critical roles in the clinical setting by providing physicians with information to guide precise treatment, monitor patient's health status and improve patient outcome.[11–13] Nucleic acid detection methods, such as polymerase chain reaction (PCR), gene sequencing and in situ hybridisation, have been constructed and applied in molecular diagnostics to detect target sequences.[14–16] However, most nucleic acid detection methods are time consuming, complex and expensive due to pretreatment, multiple reagents, labelling or complicated instrumentation. Therefore, the development of rapid and facile strategies to overcome the limitations of traditional approaches and expand the clinical utility of molecular diagnostics is essentially required.

Clustered regularly interspaced short palindromic repeats (CRISPR)-associated nuclease (Cas) are a series of nuclease proteins, guided by a single-stranded guide RNA (sgRNA), that sequence-specifically recognise the target nucleic acid.[17,18] Thus, CRISPR/Cas is an excellent tool with improved nucleic acid-targeting potential that can be used for optical detection. The detection tool has received increasing attention in recent years.[19] Since 2016, several strategies, including the NASBACC system, based on CRISPR/Cas, have been used to detect single nucleotide polymorphisms.[20] Gootenberg et al. established an RNA-targeting CRISPR/Cas13a reporting system (SHERLOCK).[21] In the strategy, the Cas13a RNP complex recognises the target RNA sequence, activating the exonuclease activity. The activation results in cleavage of a single-stranded nucleic acid probe, leading to a fluorescent output signal. Li et al. developed the HOLMES strategy.[22] In this system, a DNA-targeting CRISPR/Cas12a, instead of a CRISPR/Cas13a, is used to realise DNA sequence detection. Moreover, SHERLOCK and HOLMES can use amplification steps to further improve their sensitivities. Subsequently, other methods, such as CAS-EXPAR,[23] RCH,[24] DETECTR,[25] and gFET-CRISPR,[26] have been developed to detect different nucleic acid targets.

Biolayer interferometry (BLI) is a real-time, sensitive, and rapid analytical technique to detect biomolecular interactions by monitoring the change in the thickness of the optical biolayer.[27] Briefly, biosensors or ligands that can interact with analytes are first immobilised on the surface of BLI fibre-optic biosensors. The biomolecular interaction between the biosensor and the analyte will form a monomolecular complex layer on the BLI sensor surface and change the optical thickness, resulting in a proportional shift in the interference spectrum of reflected light. Thus, the BLI can be used to monitor biomolecular interactions in real time, as well as analyse other parameters such as association rates, dissociation rates, and

[a] Dr. S.-P. Qiao, Z.-N. Liu, Dr. H.-C. Li, H. Pan, Dr. Y.-Z. Gao
Department of Changchun Institute of Engineering Technology
Suzhou Institute of Biomedical Engineering and Technology
Chinese Academy of Science (CAS)
3333 Shengbei Street, Changchun 130052, Jilin (P. R. China)
E-mail: gaoyz@sibet.ac.cn
[b] X. He
Department of Jilin City Institute of Biological Products
Suzhou Institute of Biomedical Engineering and Technology
Chinese Academy of Science (CAS)
1228 Songjiangnan Road, Jilin 132013, Jilin (P. R. China)
[c] Dr. Y.-Z. Gao
Department of Jinan Institute of Engineering Technology
Suzhou Institute of Biomedical Engineering and Technology
Chinese Academy of Science (CAS)
3 Gangxing Road, Jinan 250000, Shandong (P. R. China)
E-mail: gaoyz@sibet.ac.cn

Supporting information for this article is available on the WWW under https://doi.org/10.1002/cbic.202100054

binding specificities.[28] This technique has been reported to be rapid and highly sensitive for analyte detection.[29] As such, the BLI technique has great potential to be explored as a targeted nucleic acid detection approach.

In this study, we prepared a biotin-modified CRISPR biosensor and constructed a nucleic acid detection strategy called CRISPR-BLI by coupling the sequence-specific CRISPR biosensor with the real-time and rapid BLI technique (Figure 1). First, the catalytically deactivated Cas9 with HaloTag (dCas9-Halo) was modified via an irreversible bond that formed between HaloTag and alkane chlorine-biotin ligand,[30] which was easily immobilised on the surface of the streptavidin-BLI sensor. Next, the dCas9-Halo-sgRNA complex (dRNP, CRISPR biosensor) interacted with the target double-stranded DNA (dsDNA) by scanning the DNA samples and hybridising with the DNA until the sequence matched with the single-guide RNA (sgRNA) of the dCas9-Halo biosensor. The specific hybridisation of the target nucleic acid to the biosensor changed the optical thickness of the BLI biolayer, resulting in a shift in the interference spectrum and optical signal output.

The CRISPR-BLI system has the combination advantages of dCas9-Halo biosensor and BLI platform. Briefly, the dCas9-Halo biosensor was prepared to consistently maintain its DNA hybridisation capability compared with the biosensor fabricated by -NH_2 or -COO modification. In addition, the highly sequence-specific CRISPR biosensor can be applied to various gene: the sgRNA of target sequence can be facilely designed and modified at 5′-end to fit nucleic acid target.[31] Meanwhile, the BLI platform has advantages of being real-time, sensitive, and rapid, as well as high-throughput because of the semiautomatic loading of the sample.[32] Therefore, the CRISPR-BLI system seems to be a promising candidate for clinical utility and nucleic acid detection.

Result and Discussion

CRISPR biosensor fabrication

dCas9-Halo protein design and purification

Several strategies such as amino or carboxyl reaction,[33,34] click chemistry,[35] Schiff base,[36] and host-guest recognition are usually attempted for labelling protein.[37] In this study, after excluding methods requiring complicated defective expression or multiple-steps, we selected three facile approaches to modify the CRISPR protein with biotin: 1) reacting biotin-sulfo-NHS ester with amino groups of proteins; 2) binding carboxyl groups on dCas9 via EDC activation; and 3) using a site-specific modification or host-guest interaction. A HaloTag-biotinylated alkane chlorine ligand was selected as the third method. The ligand and HaloTag had a high level of specific recognition and formed an irreversible bond, making this strategy facile and stable. Therefore, we designed the protein scaffold by adding a HaloTag to dCas9. Metal ion affinity and cation exchange chromatography were used to successfully purify the dCas9-Halo protein from the *Escherichia coli* BL21(ED3) cell lysate. PAGE and western blot demonstrated a high purity of dCas9-Halo (Figure S1 in the Supporting Information).

Specificity of the dCas9 to its target sequence guided by the designed sgRNA

The guiding ability of purified sgRNAs was verified through DNA cleavage test by using the PCR product (3.6 kbp) and plasmid (7.2 kbp) containing the *ALP* gene(alkaline phosphatase, GenBank: CP057634.1). Briefly, sgRNA-49 and sgRNA-1166 were incubated with the apo-Cas9 to form RNP complexes at 37 °C. Then, DNA samples of the PCR product and plasmid were combined with RNPs and incubated at 37 °C for 1 h. Figure S2

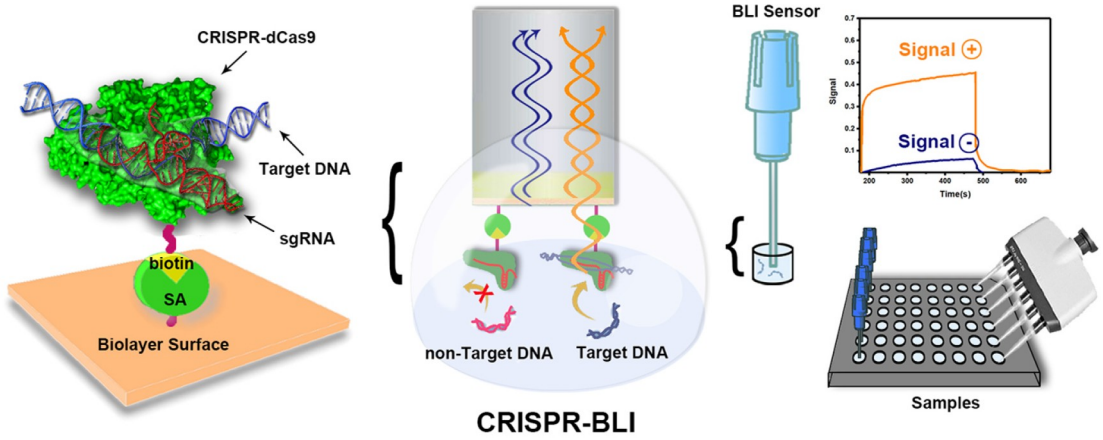

Figure 1. Illustration of CRISPR-BLI for target DNA detection. The CRISPR-BLI system integrates sequence-targeting CRISPR-Cas9 and rapid, real-time biolayer interferometry (BLI) to realise a rapid, specific, real-time detection of the target DNA. A well-labelled dCas9 complex with sgRNA (dRNP) that can specifically hybridise with the target DNA is immobilised on the surface of the BLI by the biotin-streptavidin interaction. As target DNA capturers, immobilised dRNPs recruit the target sequence by scanning and comparing sequences with sgRNA. The specific hybridisation of the target DNA to the dRNPs changes the optical thickness of the BLI biolayer, resulting in a shift in the interference spectrum and optical signal output.

demonstrates that both linear and circular target DNA were cleaved by RNPs guided by sgRNA-49 and sgRNA-1166.

The binding and specific hybridisation between target dsDNA and dRNPs were evaluated by electrophoretic mobility shift assay (EMSA), a technique for studying interaction between DNA binding proteins and associated DNA.[38] As Figure S3a illustrates, formation of dRNP-DNA complex reduces the mobility of DNA, resulting in a band shift in gel electrophoresis. EMSA in Figure S4 demonstrate significant band shift of dRNP-target DNA band compared with apo-dCas9 and DNA mixture bands in the absence of sgRNAs, revealing binding of dRNP to target dsDNA. The specific hybridisation guided by sgRNAs were also investigated by EMSA in Figure S3b, dRNP with target DNA shown a clear band shift, while no mobility changes was observed for non-specific DNA. Moreover, using nontarget PCR products of *APO* and *BNP* genes as containment, fluorescence electrophoresis (Figure S5) and western blot (Figure S6) were performed and provided the evidence of the specific hybridisation of target dsDNA to dRNP guided by sgRNAs.

Evaluation of modification methods and fabrication of the CRISPR biosensor

Protein loss and disturbing of active sites during inappropriate modification considerably decrease the protein function, limiting its further application. We selected three facile strategies for dCas9 biotinylation and investigated effect of method on function of CRISPR biosensor, establishing an optimal strategy for biosensor fabrication.

Firstly, a commoditized EZ-Link Sulfo-NHS-LC-LC-biotin was used to label apo-dCas9-Halo. Sulfo-NHS esters, which may react with primary amines (-NH_2) to form amide crosslinks, are widely used in protein labelling because of their good solubility and high coupling efficiency. In this study, different reacting ratio (molecular/ protein) were attempted and the function of modified dCas9 probe were evaluated using EMSA. Exceeded our expectations, as shown in Figure 2b, even at a ratio as low as 2:1 (0.1 times the recommend reacting ratio), the binding ability of dRNPs was considerably lower than that of unmodified dCas9. We further attempted to shorten the reaction time from 2 h to 15 min, which improved the binding of dRNPs with the target DNA; however, the biotinylation of the protein was not satisfactory according to the results obtained using the biotin quantitation kit (data not shown) and heat release of protein captured in SA-MBs (Figure S7).

Secondly, we investigated modification strategy utilizing reaction between hydrazides and carboxyl activated by EDC at pH 6.0. EMSA was performed to characterise their residual hybridisation ability of modified protein. Compared with earlier method, the EDC-induced modified biosensor demonstrated an improvement in binding ability, as shown in Figure 2c; however, the modified probe still demonstrated limitation such as low hybridisation ability (only ~50% of original dCas9) and irreversible aggregation causing by low pH.

The function of modified dCas9 were not satisfactory when using two aforementioned strategies. We assumed that the

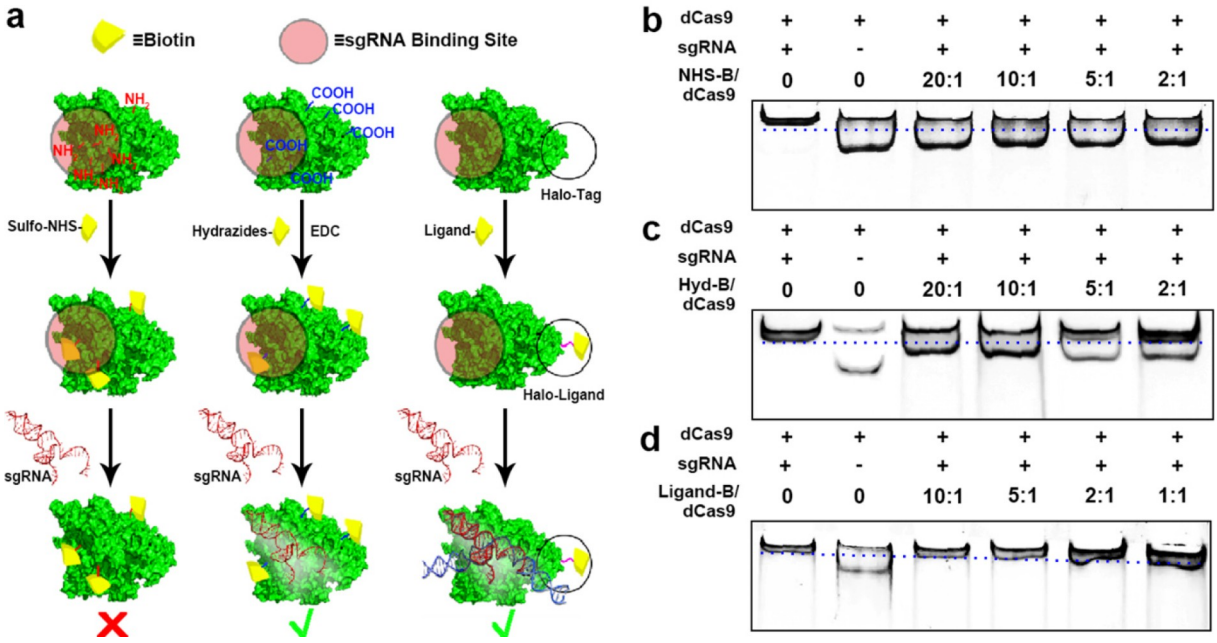

Figure 2. a) Three strategies for biotin modification of dCas9-Halo protein with specific DNA binding capacity maintained after labelling. A biosensor with good binding capacity should show a significant band shift in EMSA. Left: dCas9-Halo protein was modified with biotin by reaction with primary amines (left), carboxyl group (middle), and ligand-HaloTag recognition (right). Different strategies led to various abilities of modified dCas9 biosensor for sgRNA or DNA binding. EMSA results for evaluating the binding ability of dCas9 biosensor modified through different ratios of b) sulfo-NHS-biotin/dCas9, c) hydrazides-biotin/dCas9 and d) ligand-biotin/dCas9. Images demonstrate that dCas9 biosensor modified through ligand-HaloTag recognition has superior hybridisation capacity.

Sulfo-NHS ester preferred to react with amino acids such as asparagine, glutamine, lysine and arginine, which played a vital role in binding with sgRNA and target DNA (e.g., K913, R1333, N497, R661 Q926, as is shown in SpCas9 [PDB ID: 4UN3 and 4OO8]).[39,40] Blocking of these groups may cause space steric hindrance to be considerably large to interact with sgRNA or DNA. Similarly, modification of hydrazides may also cause a large steric hindrance when reacted with the carboxyl group located in binding pocket, resulting in a certain degree of loss of dCas9 protein's hybridisation ability (Figure 2a).

Therefore, we used the interaction between HaloTag and HaloTag PGE-biotin ligand to realise a specific modification without disturbing the sgRNA/DNA-binding pocket of dCas9. An irreversible bond formed between the HaloTag and ligand after their highly specific recognition, resulting in a facile and stable fabrication of CRISPR biosensor.[41] EMSA (Figure 2d) revealed that the CRISPR biosensor exhibited comparable hybridisation ability to which of original dCas9, which may be because of specific modification without blocking of its pocket. The CRISPR biosensor could be fabricated with adequate labelling efficiency for immobilisation even at the ratio (ligand/apo-dCas9-Halo) of 2:1, as was evidenced by the heat release of protein-captured SA-MBs (Figure S10). In summary, the HaloTag-ligand strategy demonstrated significant advance in hybridisation ability with good immobilising efficiency compared with the two earlier methods, suggesting an optimal strategy for biosensor fabrication. The residual binding ability of three biotin-modified CRISPR in Figure 2b–d is 2, 54 and 100%, respectively.

CRISPR-BLI construction

Construction of CRISPR-BLI and specific recognition to target sequence

Based on the aforementioned efforts, we attempt to construct a CRISPR-BLI platform to detect target DNA. A schematic of this experiment is shown in Figure 3a, the CRISPR-BLI chip was obtained by immobilising CRISPR biosensor on the surface of BLI via biotin streptavidin interaction. Meanwhile, plasmid with *ALP* gene were used as target DNA and PUC19 plasmid was prepared as negative control. The CRISPR(dRNP-*ALP*)-functionalised CRISPR-BLI chips were calibrated first by PBS buffer with 10 μg/mL heparin; 0.1%BSA; and 0.02% Tween-20, which have been reported to reduce nonspecific adsorption.[42] Next, chips were incubated with 800 ng of target, and nontarget DNA to evaluate the detection capacity of CRISPR-BLI. Target DNA were captured to chip surface by CRISPR biosensor, resulting in generating signal output. The response of CRISPR-BLI was recorded in real-time and analysed through OctetRED96e (BLI). Figure 3b demonstrated the real-time signal response of dRNP-

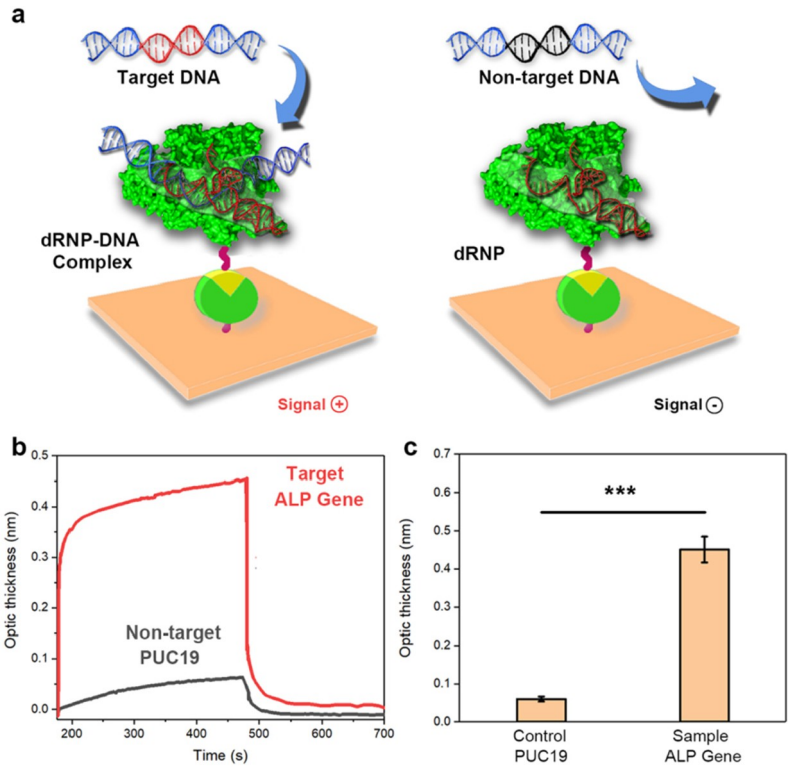

Figure 3. CRISPR-BLI specifically binds with the target DNA. a) The CRISPR-BLI was constructed by immobilising dRNP biosensors on the surface of BLI sensors. For specific binding verification, target (*ALP* plasmid) and nontarget DNA (PUC19 plasmid) samples were submitted to the dRNP-modified CRISPR-BLI chips to detect the signal. b) The real-time signal of CRISPR-BLI chips in the presence of *ALP* and PUC19 plasmid. c) The optical thickness responded signals of the CRISPR-BLI chips with target *ALP* gene were significantly higher than those of nontarget PUC19 plasmid (***$P < 0.0002$, two-tailed t-test, $n = 3$). CRISPR-BLI demonstrated the ability for specific detection of DNA samples. Error bars represent standard deviation.

sgRNA49-functionalised CRISPR-BLI platform in the presence of target *ALP* and nontarget sequence. The signal output of target DNA was significantly larger than that of nontarget negative control (PUC19 plasmid, 800 ng; Figure 3c). This finding demonstrated that the signal of the CRISPR-BLI chip is sequence-specific due to the specific hybridisation of CRISPR biosensor with target sequence. Furthermore, the DNA-association and disassociation of CRISPR-BLI chip occurred rapidly within 9 min (Figure 3b), suggesting that the CRISPR-BLI system is a promising candidate for clinical utility and nucleic acid detection.

Affinity of the immobilised CRISPR to its target DNA

To ensure that the signal response come from specific binding of immobilised CRISPR to target DNA, we verified the affinity of immobilized CRISPR biosensor to target sequence by using streptavidin-modified magnetic beads (MBs-SA) as solid phase. (Figure 4) Biotinylated apo-dCas9 were first immobilised onto MBs-SA using the same immobilisation protocol as CRISPR-BLI chip modification and then assembled with *ALP*-specific sgRNA to form the dRNP-*ALP* complex. The affinity of immobilised CRISPR biosensor was thus characterised by the capture efficiency of MBs-dRNP-*ALP* DNA capturer. After incubating with MBs-dRNP-*ALP* for 1 h and magnetic separation, the DNA concentration of pre- and post-incubation supernatant were analysed via gel electrophoresis (Figure 4b) to evaluate capture efficiency and relative affinity between immobilised CRISPR sensor and target DNA. Meanwhile, nontarget plasmid (PUC 19) was also incubated and extracted by MBs-dRNP-*ALP* complex as negative control. The efficiency of MBs-dRNP-*ALP* complex for capturing *ALP* DNA was significantly higher than that of PUC19 control (Figure 4c). These results demonstrated that the immobilised CRISPR biosensor maintain high specific affinity to target DNA sequences and retain as stable hybridisation even under physical force of wash, vortex and ultrasonic. This finding provides another evidence that CRISPR-BLI generates signal output through specific hybridisation rather than other non-specific binding.

Evaluation of immobilised dRNPs biosensors for quantitative analysis using the fluorescence test

The ability of immobilised CRISPR for quantitative analysis was next investigated via fluorescence measurement. As schematic of this experiment shown in Figure S12a, the MBs-dRNP captured the target DNA, which further hybridised with free FITC-labelled-dRNP, resulting in fluorescence decline of solution. Briefly, MBs-dRNP (sgRNA-1166) were first prepared with same protocol as described earlier. Meanwhile, a type of FITC-dRNP (sgRNA-49) was also fabricated as fluorescence reporter. For fluorescent quantitative analysis, MBs-dRNP, DNA, and FITC-dRNP were first mixed and incubated at 37 °C, and the

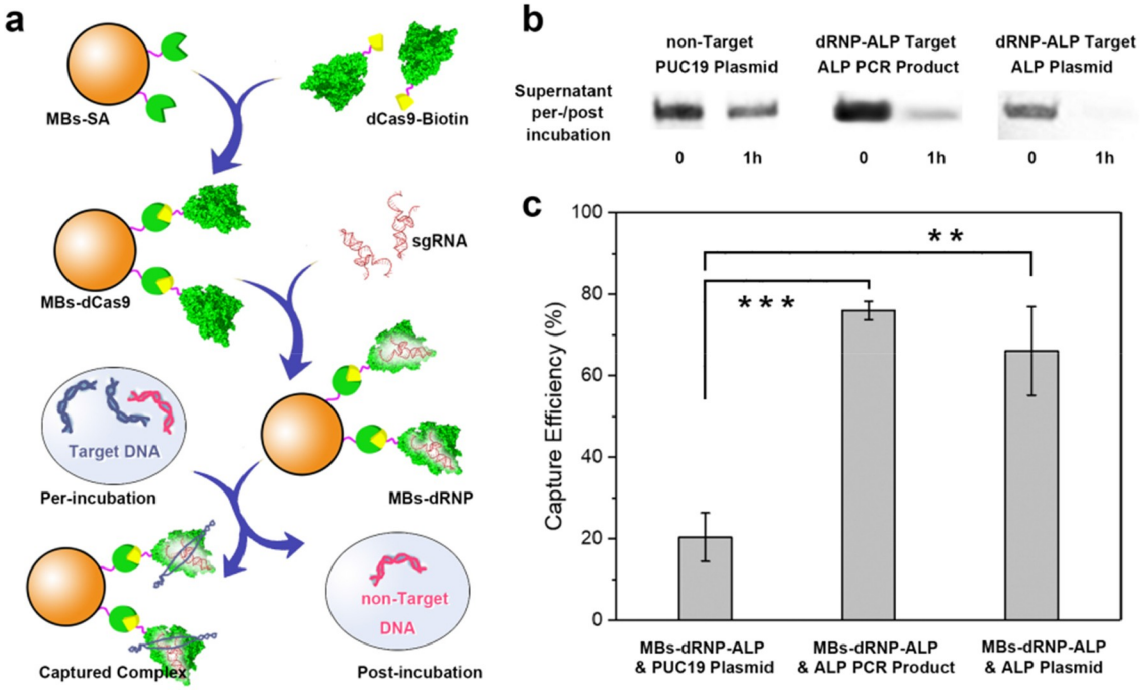

Figure 4. The sequence-targeting dRNP biosensor effectively binds the specific target DNA. a) dCas9-functionalised SA-MBs were obtained to evaluate the specific binding ability of the immobilised dRNP to its target DNA samples. The dCas9 protein was first immobilised to SA-MBs through biotin-streptavidin interaction, then sgRNA was added and assembled with dCas9 to form the MBs-dRNP capturer. Finally, DNA samples were mixed with MB-dRNP and incubated at 37 °C for 1 h. b) The supernatant of samples before and after incubation was analysed by gel electrophoresis and ImageJ to evaluate the capture efficiency of MB-dRNP capturer to target *ALP* DNA and nontarget PUC19. c) The immobilized dRNP demonstrated significantly higher capture efficiency for target *ALP* DNA (~76% for *ALP* PCR products and ~65% for *ALP* plasmid) than nontarget PUC19 plasmid (***$P < 0.0002$, **$P = 0.004$, two-tailed t-test, $n = 3$), revealing that the immobilized dRNP still maintained its specific affinity to target DNA. Error bars represent standard deviation.

fluorescence intensity of supernatant was monitored[43] by microplate reader (Tecan) during incubation. All fluorescence measurement were performed in solution with salmon sperm DNA and heparin, which as nontarget DNA and non-specific-bind inhibitor, respectively. As demonstrated in Figure S12b and c, the *D* value of fluorescence dropped with the increasing time and presented linear calibration curve with DNA in the range from 0 to 600 ng. A slight fluorescence reduction of negative control (0 ng) was also observed (< 9.1 %) possibly because of the volume change and the tiny nonspecific binding between FITC-dRNP and MBs. These findings reveal an evidence that immobilised CRISPR biosensor could be used for quantitative analysis of target DNA.

DNA detection based on CRISPR-BLI

Evaluation of CRISPR-BLI for detection of target sequence

Based on the construction of CRISPR-BLI platform, we further investigated its quantitative ability to detect target DNA. As Figure 5a demonstrated, the real-time signal of dRNP-*ALP*-immobilised CRISPR-BLI chips was recorded in the presence of varying concentrations of *ALP* plasmid (25–800 ng), meanwhile, 800 ng of the PUC19 sample was incubated with the same type of chip for assessing the specific detection ability. The two CRISPR-BLI chips

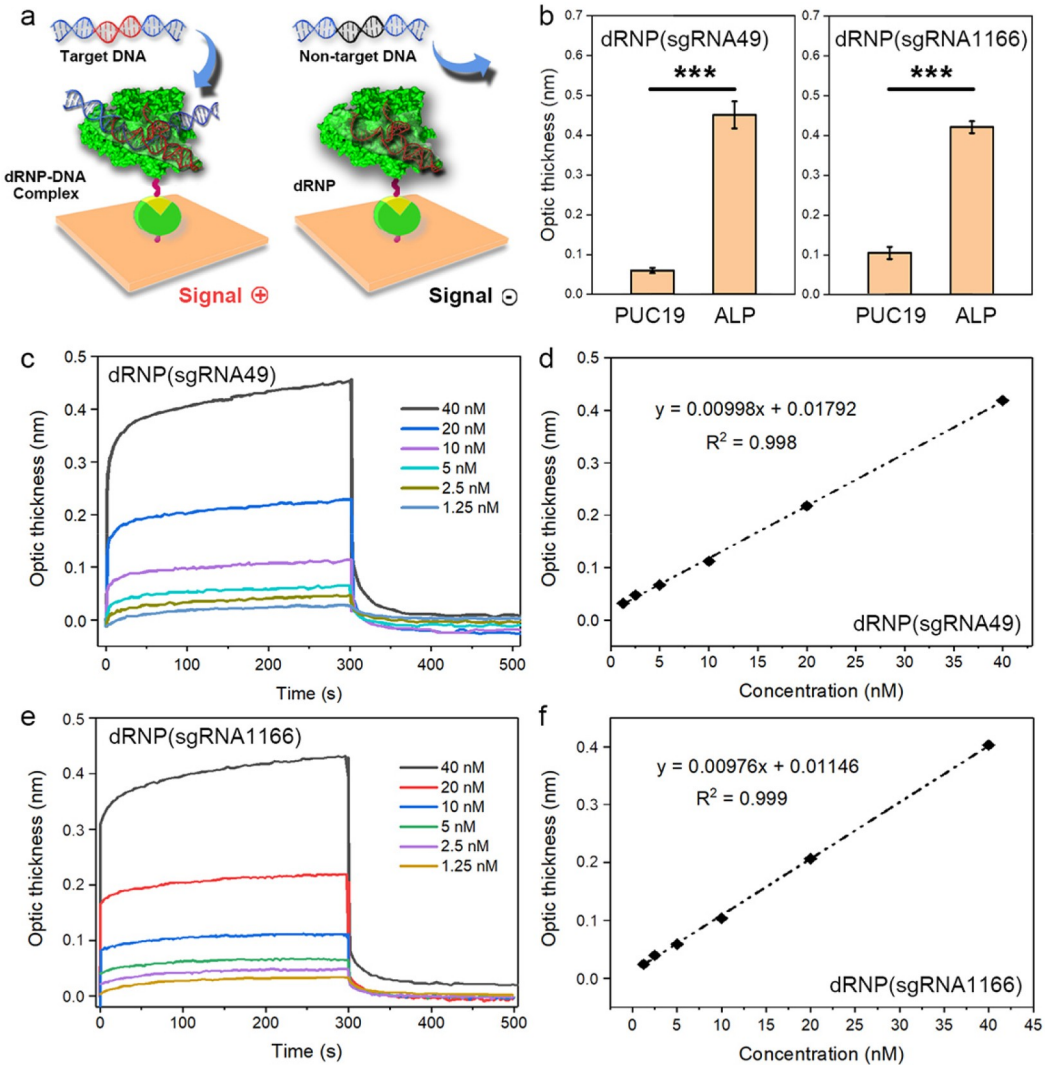

Figure 5. CRISPR-BLI could realise specific and quantitative analysis of target DNA samples. a) Scheme for the CRISPR-BLI response to samples in the presence of target (left) and nontarget (right) DNA. b) Specific signals of CRISPR-BLI modified with dRNP (sgRNA49) (left) and dRNP (sgRNA1166) (right); both dRNP-immobilised chips demonstrated significantly higher signal output when they were used to detect the *ALP* gene compared with the nontarget sequence (***$P < 0.0002$, two-tailed t-test, $n = 3$). Error bars represent standard deviation. c) Real-time signal output of dRNP (sgRNA49)-modified CRISPR-BLI in the presence of various concentrations of the *ALP* gene during the association and dissociation process. d) The dRNP (sgRNA49)-modified CRISPR-BLI calibration curve with different concentrations of the *ALP* gene. Linear fitting ranged from 1.25 to 40 nM, and R^2 is the determination coefficient. e) Real-time signal output of dRNP (sgRNA1166)-modified CRISPR-BLI in the presence of various concentrations of the *ALP* gene during the association and dissociation processes. f) The dRNP (sgRNA1166)-modified CRISPR-BLI calibration curve with different concentrations of the *ALP* gene. Linear fitting ranged from 1.25 to 40 nM, and R^2 is the determination coefficient.

demonstrated a significant enhancement in the signal output after incubation with 800 ng of *ALP* plasmid compared with the negative control (Figure 5b). This finding demonstrated that CRISPR-BLI chip is a specific detection method. Although both dRNP-*ALP*-modified CRISPR-BLI chips demonstrated a positive correlation with *ALP*-plasmid, the dRNP-sgRNA49-functionalised-CRISPR-BLI exhibited as a better chip given the similar response (~0.451 nm) and higher specificity (~13.9% unspecificity) compared with the one functionalised with dRNP-sgRNA1166 (~0.455 nm, ~16% unspecificity). The real-time signal response of two CRISPR-modified CRISPR-BLI chips with varying concentrations of *ALP*-plasmid is detailed in Figure 5c and e. The sensitivity of dRNP-sgRNA49- and dRNP-sgRNA1166-modified chips for *ALP* DNA detection was evaluated. The limit of detection were 863.4 and 941 pM (1.9 and 2.0 ng μL^{-1}, considering the molecular weight of *ALP* plasmid, ~2.1×10^6 g mol^{-1}), respectively (Figure 5d and f), according to the equation:[44]

$$\mathrm{LOD} = 3\delta/k \quad (1)$$

where δ is the standard deviation of the signal response of the negative control and k is the slope of the calibration curve. In addition, the real-time signal output, as shown in Figure 6, indicated that the signal almost reached its saturation within 5 min of the incubation of the chip with the sample, suggesting that this incubation time is adequate to capture the target DNA. The complete CRISPR-BLI analysis process, including biosensor immobilisation, sample analysis, and the dissociation step, was completed in 23 min (Scheme S2). Meanwhile, the semiautomatic analysis of BLI samples loaded on 96-well plates demonstrated better throughput. This finding revealed that CRISPR-BLI is a rapid and high-throughput strategy for target DNA detection that can be practically applied for clinical needs. Moreover, other parameters such as K_d, K_{on} (1/Ms), and K_{dis} (1/s), which reveal the affinity of dRNPs to the target DNA, were also calculated through CRISPR-BLI (Table S4). These parameters could be used for scanning and evaluating off-target efficiency of the designed sgRNA in vitro, demonstrating its application in not only clinical detection but also academic research.

Construction and evaluation of signal-amplified CRISPR-BLI by coupling PCR amplification for target sequence detection

To further improve sensitivity of CRISPR-BLI chip, we attempted to combine CRISPR-BLI with PCR, which is a preferred strategy to amplify and improve signal output of nucleic acid

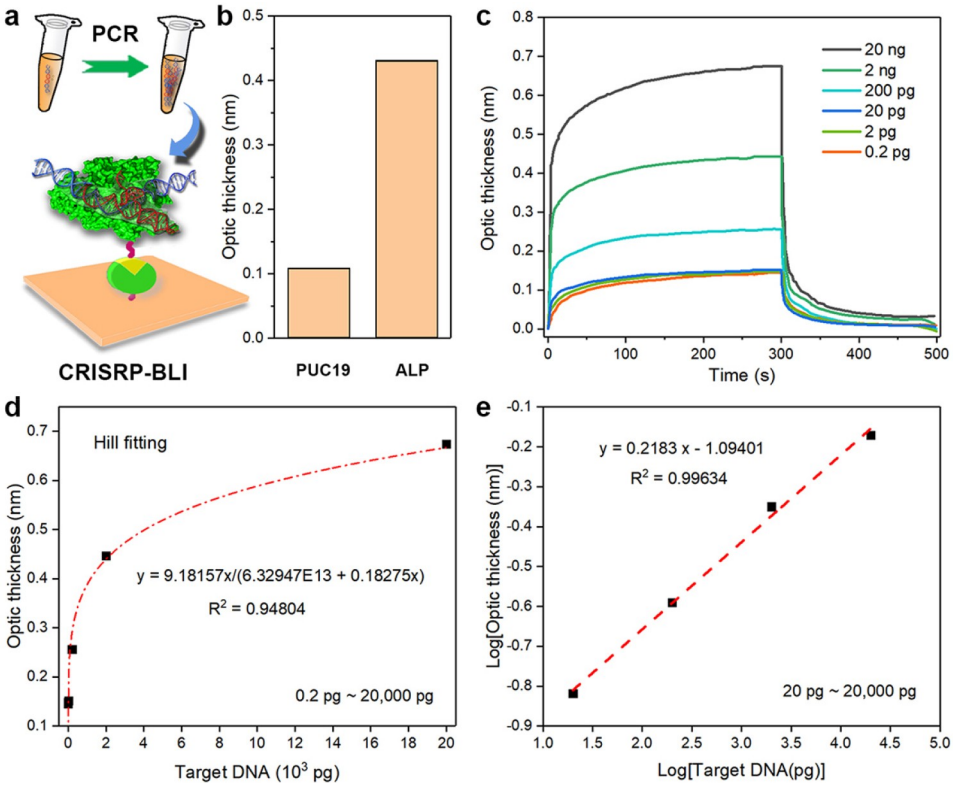

Figure 6. Construction of the PCR-coupled CRISPR-BLI system for improving the sensitivity of target DNA detection. a) Scheme for PCR-coupled CRISPR-BLI. Target DNA was first amplified by 15-cycle PCR and directly analysed with dilution. b) Specific signals of PCR-coupled CRISPR-BLI modified with dRNP (sgRNA49) in the presence of PCR solution using *ALP* and PUC19 as templates. The target *ALP* groups still demonstrated significantly higher signal output than that of the nontarget sequence. c) Real-time signal output of dRNP (sgRNA49)-modified PCR-coupled CRISPR-BLI in the presence of various amounts of *ALP* (count by original template). d) The PCR-coupled CRISPR-BLI calibration curve with different amounts of the *ALP* gene. Hill fitting ranged from 0.2 pg to 20 ng, and R^2 is the determination coefficient. e) PCR-coupled CRISPR-BLI sensitivity calibration curve (log[signal] vs. log[target DNA amount (count by original template)]). Linear fitting ranged from 20 pg to 20 ng, and R^2 is the determination coefficient. The sensitivity was improved through DNA amplification.

detection. First, we constructed a PCR model for optimising the reaction conditions. Meanwhile, we selected a suitable amplification cycle number at which the target DNA was appropriately amplified in the least time to decrease the total time of detection as much as possible. Briefly, a 3.6 kbp PCR product containing the *ALP* gene was obtained (Figure S13) through PCR by using a pair of primers that matched with the *ALP*-plasmid. Based on this, fluorescent qPCR reactions were performed following the addition of 0.5×SYBR Green I in the presence of varying quantities of the *ALP*-plasmid template (from 0.2 pg to 200 ng). The real-time signal output was monitored and analysed by the MyGo PCR system to determine a suitable amplification cycle number. As shown in Figure S14, the signal of samples demonstrated a typical qPCR pattern and increased rapidly during 5–20 cycles. For quantitative detection of the target DNA by using the least amplification time, we selected the 15th cycle as the suitable time point as it balanced better fluorescent intensity of amplified DNA and was less time consuming.

With a similar protocol as mentioned earlier, the detection ability of signal amplified CRISPR-BLI was verified by using dRNP-sgRNA49 that targeted the middle location of the 3.6 kbp PCR products and demonstrate better response to target DNA. As illustration in Figure 6a, Samples containing varying quantity of target sequence were first amplified through a 15-cycle PCR reaction. The PCR products were then diluted twice and analysed by CRISPR-BLI chip to evaluate the sensitivity of PCR-coupled CRISPR-BLI system. Meanwhile, negative control was prepared through a 15-cycle PCR using 200 ng of PUC19 as template.

As is shown in Figure 6, the capacity of the quantitative analysis of dRNP-sgRNA-49-immobilised CRISPR-BLI in the presence of 3.6 kbp PCR products was demonstrated. The signal output of CRISPR-BLI chips rapidly responded to the addition of PCR products and exhibited a wide positive correlation with the DNA template, ranging from 0.2 to 20000 pg via the Hill fitting ($R^2 = 0.9480$; Figure 6d). For calculating the LOD of PCR-coupled CRISPR-BLI, we first obtained a linear calibration curve by performing a logarithmic operation to the input DNA amount and output signal (log[DNA] vs log[BLI signal]). The linear range of PCR-coupled CRISPR-BLI was 20 to 20000 pg ($R^2 = 0.9963$; Figure 6e), and the LOD was 1.34 pg according to the equation:[45]

$$S/N = 3 \quad (2)$$

where S is sensitivity's logarithm of the BLI system, and N is the standard deviation of the logarithm of the signal output of the negative control (see the Supporting Information). Moreover, as shown in Figure S15, the baseline of the negative control in PCR-coupled CRISPR-BLI was about two times higher than that of the first-generation CRISPR-BLI using the PUC19 plasmid as control. We speculated that this result may be due to the nonspecific adsorption between BLI sensors and complex composition of the PCR reagent, such as polymerase protein and high concentration of reaction substrates or primers. The time consumed for target sequence detection of the PCR-coupled CRISPR-BLI system was optimised to 90 min, containing an 80-min 15-cycle PCR amplification process and a 10-min step for real-time signal readout.

Although we successfully constructed the CRISPR-BLI for target DNA detection, more insights are required into a few aspects, warranting further studies. First, the completion time for the PCR-coupled CRISPR-BLI approach is still time consuming. Isothermal amplification technology, which is more rapid and facile, can substitute PCR methods to shorten the time. Second, instead of nucleic acid amplification, the detection sensitivity could be improved by using other signal-amplified strategies. 1) Optimisation of the immobilisation density of the dCas9 probe, 2) use of DNA-binding substrate or protein or synthesising larger complex to increase the optical thickness changes.

Conclusion

In this study, we explored a modification strategy that could highly maintain the specific hybridisation ability of CRISPR-Cas to recognise nucleic acids. The immobilised CRISPR biosensor was used as a capturer to establish a CRISPR-BLI system for facile, rapid, specific, and real-time identification and quantification of target dsDNA. The CRISPR-BLI system is an attractive approach due to not only the rapid, label-free, and real-time properties of the BLI but also the high affinity and specificity of the CRISPR biosensor.

The specific and quantitative detection ability of CRISPR-BLI chip was characterised in this study. Although the CRISPR-BLI chip was designed to specifically detect only *ALP*-plasmid as mimics of genetic analyte, it indicates that the CRISPR-BLI platform can be expanded for analysis of large and complex genomic materials by easily varying the sgRNA sequence or modification.[31] The LOD of the CRISPR-BLI chip was found to be 863.4 pM (1.9 ng μL^{-1}) without amplification, which is comparable with amplification-free technologies reported previously.[46,47] A comparison of technologies is detailed in Table S5. According to these findings, a new-generation CRISPR-BLI was constructed by coupling the PCR amplification method. Through a 15-cycle PCR, the sensitivity of PCR-coupled CRISPR-BLI was improved to 1.34 pg with a linear range from 20 to 20000 pg. Although increasing its amplification cycle could further improve its sensitivity, it would affect the quantitative range and extend the detection time. Fitting in with the CRISPR-BLI chip, a signal amplification strategy named DNA cascade reaction (DCR)[48–50] could be further explored and applied in this CRISPR-BLI system. With well design of DCR, the chip signal could be improved because of signal improvement of BLI caused by the "on-chip" enhancement of target DNA. Compared with reported strategies such as gold nanoparticle microarrays and surface plasmon imaging with multiple steps,[51] CRISPR-BLI chip was facile in requirement of multiple treatment, reagents, and equipment.[52] Meanwhile, by semiautomatic loading and analysis of BLI system, samples were reported with a satisfying throughput through a digital signal readout that is accurate, rapid, and obtained in real time. However, it is still

time consuming for PCR amplification, and PCR samples demonstrate a higher nonspecificity in the PCR-CRISPR-BLI. The limitations may be solved with the developed isothermal amplification and rapid DNA purification technologies to promote application of CRISPR-BLI.

The CRISPR-BLI system not only performs qualitative and quantitative detection of the target DNA but also provides affinity parameters based on the BLI platform (Table S4). This system can be used to evaluate the affinity of sgRNA to Cas protein and RNP complex to target/off-target nucleic acids by measuring the association-dissociation kinetics. As such, the CRISPR-BLI system can be used as a tool for validation and evaluation of RNP efficacy and target-off-target prediction in vitro, suggesting its utility in academic settings. Overall, the CRISPR-BLI system, a sequence-specific CRISPR-Cas coupled with and rapid, real-time BIL technology, is a promising tool for target DNA detection. Further studies can be focused on fabrication of various types of biosensors such as Cas13a and Cas14, to satisfy the practical clinical application of CRISPR-BLI in analysis of various genetic materials (e.g., genomic nucleic acid, nucleic acid from virus).

Experimental Section

Expression and purification of dCas9-Halo protein: The gene containing dCas9 (deactivated CRISPR/Cas9 from *Streptococcus pyogenes* with D10A and H840A mutations; Sequence 1 in the Supporting Information) and Halo tag were obtained from the pET302-6His-dCas9-Halo plasmid (Addgene) and cloned into PET-16b containing an N-terminal hexahistidine tag. *E. coli* BL21(ED3) cells (Sangon Biotech Co. Ltd.) were used to express protein. Cells were cultured in LB medium containing 100 $\mu g\,mL^{-1}$ ampicillin, followed by addition of isopropyl β-D-thiogalactopyranoside (IPTG; Sigma) to a final concentration of 0.25 mM. For purification, the cell lysate was first applied to the 5 mL Nuvia IMAC metal affinity column (Bio-Rad) in 50 mM PBS buffer. The eluted protein was purified further through a cation ion-exchange column (HiTrap SP; GE Healthcare) and stored at −80 °C with 20% (*v/v*) glycerol until use.

Single-guide RNA (sgRNA) design and synthesis: ALP gene from *E. coli* DH5α is used as model analyte. sgRNA was designed using software (http://crispr.tefor.net/crispor.py). Two sgRNAs, sgRNA-49 and sgRNA-1166, were selected (Sequences 4 and 5). Briefly, the DNA template was first obtained by PCR amplification of splint ligation of two synthetic single-strand nucleotides (Scheme S1). Single-strand nucleotides, primers (Sangon Biotech Co. Ltd.) and the PCR system are illustrated in the Supporting Information. Purified using TIANquick Maxi Purification Kit (Tiangen Biotech Co. Ltd.), the linear DNA template was used to synthesise sgRNA in vitro with T7 RNA polymerase kit (NEB). The obtained sgRNA was purified using RNAclean Kit (Tiangen Biotech Co. Ltd.), and verified through DNA cleavage test using Cas9 (NEB).

Fabrication of dCas9 biosensor: For dCas9-NHS-biotin, EZ-Link Sulfo-NHS-LC-LC-biotin (A35358; Thermo Scientific) was dissolved and mixed with the dCas9-Halo protein (1–2 mg/mL) in different ratios (from 2:1 to 20:1) and incubated on ice for 2 h. The excessive unreacted molecules were removed through Zeba spin desalting columns (89882, Thermo Scientific). The final dCas9-NHS-biotin was concentrated and stored at −80 °C until use.

For dCas9-acylhydrazine-biotin, biotin-LC-hydrazides (Sangon Biotech Co. Ltd.) reacted with the carboxyl groups of dCas9 activated by 1-ethyl-3-(3-dimethylaminopropyl) carbodiimide hydrochloride (EDC·HCl; BBI). Briefly, biotin-LC-hydrazides and EDC were freshly dissolved in 50 mM MES ((2-*N*-morpholino)ethanesulfonic acid; BBI buffer, pH 6.0). The dCas9 was mixed with biotin-LC-hydrazides (1.25 mM) and EDC (6.5 mM) and incubated at room temperature for 4 h. Next, the biotinylated protein was applied to desalting columns to remove excessive unreacted molecules. The dCas9-acylhydrazine-biotin was finally stored at −80 °C until use.

For dCas9-Halo labelling, HaloTag PGE-biotin ligand (G859B, Promega) was added to the protein in a 2:1 ratio. Biotinylated dCas9-Halo was allowed to react at room temperature for 1 h and incubating overnight at 4 °C, after which it was treated with 40-K MWCO Zeba spin desalting columns to remove excessive unreacted ligand molecules. The obtained dCas9-Halo-biotin was stored at −80 °C until use.

Electrophoretic mobility shift assay: dCas9 protein and biotinylated biosensors (1 μg) were mixed with the synthesised sgRNA (2 μg) in 50 mM HEPES (pH 7.5), 150 mM NaCl, 2 mM $MgCl_2$, 0.05% BSA (*w/v*), and 20 μg/mL heparin (BBI) at 37 °C for 15 min, followed by addition of the plasmid containing the cloned *ALP* gene and incubation at 37 °C for another hour. Samples were loaded onto 5% non-denaturing polyacrylamide gel (1×TEB buffer, 20 μg/mL heparin) and submitted to electrophoresis at 110 V for 80 min. The gel was then stained by 2×GeneGreen (Tiangen Biotech Co. Ltd.) and Coomassie Blue R25 (Sangon Biotech Co. Ltd.) to analyse the specific interaction between the CRISPR protein and target DNA.

Affinity of dCas9-ALP-SA-MBs towards DNA containing the ALP gene: Streptavidin-modified magnetic beads (SA-MBs; 1.0 μm; Dynabeads MyOne Streptavidin C1; Invitrogen) were washed three times and mixed with CRISPR proteins at a mass ratio of 500:30. The mixture containing 60 μg/mL dCas9 protein in PBS was kept at room temperature for 1 h to allow CRISPR biosensor coupling. Then, SA-MBs were blocked with 1% *w/v* bovine serum albumin (BSA; BBI) and 1.0 M glycine (Sigma) at room temperature for 1 h and washed five times. The final complex was prepared by further incubating dCas9-coupled SA-MBs (0.5 mg/mL) with *ALP*-related sgRNAs (30 ng/μL) at 37 °C for 30 min. To evaluate the affinity of each dCas9 to target DNA, the dCas9-*ALP*-SA-MB complex (500 μg) was mixed with 100 ng of the *ALP*-containing plasmid (100 μL; 7.2 kbp) and incubated at 37 °C for 1 h. The supernatant of the samples was analysed using gel electrophoresis (60 V for 30 min), and ImageJ (National Institutes of Health). Meanwhile, the PUC19 plasmid served as the control group. Experiments for measuring affinity of functionalised SA-MBs towards DNA were repeated three times. The specific capture of target DNA was demonstrated by comparing capture efficiency of target DNA and negative control using two-tailed t-test.

Evaluation of dCas9 biosensor through fluorescence analysis: The dCas9 protein coupled with sgRNA-49 was labelled by FITC as a fluorescence reporter. Cas9-Halo-sgRNA-1166 functionalised SA-MBs (50 μg) were mixed with a solution containing fluorescence reporter (5 μg), target DNA containing the *ALP* gene (0–600 ng), and nontarget DNA (50 μg; salmon sperm DNA; BBI) in PBS (20 mM PBS, pH 7.0; 20 μg/mL heparin; 2 mM EDTA; 2 mM KF) at 37 °C. The fluorescence of the obtained supernatant was recorded using a microplate reader (Infinite® M1000 Pro; Tecan) within 220 min. The decreased fluorescence intensity was used to evaluate the specific hybridisation of the dCas9-Halo biosensor and target DNA. Each sample in experiments were analysed three times with different Cas9-Halo-sgRNA-1166 functionalised SA-MBs. The correlation test of fluorescence decline to DNA amount was undertaken with the linear correlation analysis.

Construction and evaluation of the CRISPR-BLI system: The CRISPR-BLI system was constructed by immobilising biotinylated dCas9-Halo biosensor with sgRNA onto SA biosensors (ForteBio), and the target DNA was detected in the solution by using the Octet RED96e BLI System (ForteBio). Buffer, biosensor, and analytes were placed in a 96-well plate (flat bottom, black polypropylene microplate; Greiner), as shown in Tables S2 and S3. SA biosensors were first installed and dipped into the PBS buffer for 60 s to equilibrate signal as baseline. Next, an association step was run, wherein the SA biosensors were dipped into the dCas9-Halo solution (20 μg/mL) diluted by the PBS buffer to load the biosensor (dCas9-Halo-sgRNA; dRNP) for 880 s. After equilibrating the SA biosensors in the PBS buffer for another 180 s, CRISPR-BLI sensors were ready to use and were dipped into samples for 300 s for hybridisation and analysis of the target DNA. Finally, a dissociation step was performed for 200 s to dissociate the analytes in the PBS buffer. Samples with target sequence (0–40 nM) were analysed using the CRISPR-BLI system Meanwhile, samples with the nontarget DNA were also applied to CRISPR-BLI to evaluate non-specific binding. This detection system is rapid as the whole process is completed within 30 min (Scheme S2). Experiments in these studies were performed with three different CRISPR-BLI chips for each sample analysis, The specific binding of target DNA was investigated by comparing signal output of target DNA and negative control using two-tailed t-test. The sensitivity of CRISPR-BLI was investigated by correlation test using linear fitting.

PCR amplification of the ALP gene: The PCR reaction was designed and performed to amplify the target DNA. Primers used for the *ALP* gene amplification were shown in Table S1. PCR with different concentrations of the template was executed for 25-cycle amplification, the details of which are presented in Supporting information. The PCR product was analysed using gel electrophoresis (60 V for 30 min) stained with 1X GeneGreen (Figure S10). A qPCR test with a 45-cycle amplification step was performed in the presence of 0.5× SYBR Green I (SR4110, Solarbio Life Science) under the same condition of PCR and monitored by MyGo PCR systems (IT-IS Life Science Ltd.).

Evaluation of CRISPR-BLI detection combine with PCR amplification: The samples underwent a pre-PCR amplification step containing 15 cycles. During the time, dRNP biosensors were immobilised onto the surface of the BLI sensor to construct the CRISPR-BLI platform. The PCR products were diluted two times by using PBS, and loaded onto 96-well microplates for performing high-throughput CRISPR-BLI assay. The PCR-CRISPR-BLI analysis was performed in the same way as CRISPR-BLI detection under the following conditions: baseline, 180 s; detection, 300 s; and dissociation, 200 s, with all assay steps executed at 37 °C. The sensitivity of PCR-CRISPR-BLI was investigated via correlation test, detail information were shown in the Support Information for LOD calculation.

Acknowledgements

This study was supported by grants from Science and Technology Development Planning of Jilin Province (grant no. 20180201060YY), and Science and Technology Development Planning of Jilin Province (grant no. 20190303110SF).

Conflict of Interest

The authors declare no conflict of interest.

Keywords: biolayer interferometry · CRISPR · dCas9 modification · DNA detection

[1] C. S. Pareek, R. Smoczynski, A. Tretyn, *J. Appl. Genet.* **2011**, *52*, 413–435.
[2] G. Iyer, A. J. Hanrahan, M. I. Milowsky, H. Al-Ahmadie, S. N. Scott, M. Janakiraman, M. Pirun, C. Sander, N. D. Socci, I. Ostrovnaya, A. Viale, A. Heguy, L. Peng, T. A. Chan, B. Bochner, D. F. Bajorin, M. F. Berger, B. S. Taylor, D. B. Solit, *Science* **2012**, *338*, 221.
[3] N. Waddell, M. Pajic, A. M. Patch, D. K. Chang, K. S. Kassahn, P. Bailey, A. L. Johns, D. Miller, K. Nones, K. Quek, M. C. Quinn, A. J. Robertson, M. Z. Fadlullah, T. J. Bruxner, A. N. Christ, I. Harliwong, S. Idrisoglu, S. Manning, C. Nourse, E. Nourbakhsh, S. M. Grimmond, *Nature* **2015**, *518*, 495–501.
[4] D. Wu, H. Xu, H. Shi, W. Li, M. Sun, Z. S. Wu, *Anal. Chim. Acta* **2017**, *957*, 55–62.
[5] M. L. Ermini, S. Mariani, S. Scarano, M. Minunni, *Biosens. Bioelectron.* **2013**, *40*, 193–199.
[6] Y. P. Bao, M. Huber, T. F. Wei, S. S. Marla, J. J. Storhoff, U. R. Müller, *Nucleic Acids Res.* **2005**, *33*, e15-e15.
[7] A. Beyer, S. Pollok, A. Rudloff, D. Cialla-May, K. Weber, J. Popp, *Macromol. Biosci.* **2016**, *16*, 1325–1333.
[8] Y. Li, S. Li, J. Wang, G. Liu, *Trends Biotechnol.* **2019**, *37*, 730–743.
[9] B. R. Korf, H. L. Rehm, *Jama* **2013**, *309*, 1511–1521.
[10] D. S. Chertow, *Science* **2018**, *360*, 381–382.
[11] Y. Huang, Y. L. Zhang, X. M. Xu, J. H. Jiang, G. L. Shen, R. Q. Yu, *J. Am. Chem. Soc.* **2009**, *131*, 2478–2480.
[12] H. F. Dong, W. C. Gao, F. Yan, H. X. Ji, H. X. Ju, *Anal. Chem.* **2010**, *82*, 5511–5517.
[13] J. Huang, Y. Wu, Y. Chen, Z. Zhu, X. Yang, C. J. Yang, K. Wang, W. Tan, *Angew. Chem. Int. Ed.* **2011**, *50*, 401–404; *Angew. Chem.* **2011**, *123*, 421–424.
[14] a) W. J. Ansorge, *New Biotechnol.* **2009**, *25*, 195e203; b) "Novel Next-Generation DNA Sequencing Techniques for Ultra-High-Throughput Applications in Bio-medicine", W. J. Ansorge in *Molecular Diagnostics, Vols. 365–378*, 2nd ed. (Eds.: G. Patrinos, W. J. Ansorge), **2010**, p. 365.
[15] M. Li, N. Brenwald, S. Bonigal, K. Chana, H. Osman, B. Oppenheim, *J. Infect.* **2012**, *65*, 60e63.
[16] A. Markou, A. Strati, N. Malamos, V. Georgoulias, E. S. Lianidou, *Clin. Chem.* **2011**, *57*, 421e430.
[17] S. Y. Li, Q. X. Cheng, J. K. Liu, X. Q. Nie, G. P. Zhao, J. Wang, *Cell Res.* **2018**, *28*, 491–493.
[18] J. S. Chen, E. Ma, L. B. Harrington, M. Da Costa, X. Tian, J. M. Palefsky, J. A. Doudna, *Science* **2018**, *360*, 436–439.
[19] A. East-Seletsky, M. R. O'Connell, S. C. Knight, D. Burstein, J. H. Cate, R. Tjian, J. A. Doudna, *Nature* **2016**, *538*, 270–273.
[20] K. Pardee, A. A. Green, M. K. Takahashi, D. Braff, G. Lambert, J. W. Lee, T. Ferrante, D. Ma, N. Donghia, M. Fan, N. M. Daringer, I. Bosch, D. M. Dudley, D. H. O'Connor, L. Gehrke, J. J. Collins, *Cell* **2016**, *165*, 1255–1266.
[21] J. S. Gootenberg, O. O. Abudayyeh, J. W. Lee, P. Essletzbichler, A. J. Dy, J. Joung, V. Verdine, N. Donghia, N. M. Daringer, C. A. Freije, C. Myhrvold, R. P. Bhattacharyya, J. Livny, A. Regev, E. V. Koonin, D. T. Hung, P. C. Sabeti, J. J. Collins, F. Zhang, *Science* **2017**, *365*, 438–442.
[22] S. Y. Li, Q. X. Cheng, J. M. Wang, X. Y. Li, Z. L. Zhang, S. Gao, R. B. Cao, G. P. Zhao, J. Wang, *Cell Discov.* **2018**, *4*, 20.
[23] M. Huang, X. Zhou, H. Wang, D. Xing, *Anal. Chem.* **2018**, *90*, 2193–2200.
[24] X. Y. Qiu, L. Y. Zhu, C. S. Zhu, J. X. Ma, T. Hou, X. M. Wu, S. S. Xie, L. Min, D. A. Tan, D. Y. Zhang, L. Zhu, *ACS Synth. Biol.* **2018**, *7*, 807–813.
[25] J. S. Chen, E. Ma, L. B. Harrington, M. Da Costa, X. Tian, J. M. Palefsky, J. A. Doudna, *Science* **2018**, *360*, 436–439.
[26] R. Hajian, S. Balderston, T. Tran, T. deBoer, J. Etienne, M. Sandhu, N. A. Wauford, J. Y. Chung, J. Nokes, M. Athaiya, J. Paredes, R. Peytavi, B. Goldsmith, N. Murthy, I. M. Conboy, K. Aran, *Nat. Biomed. Eng.* **2019**, *3*, 427–437.
[27] J. Concepcion, K. Witte, C. Wartchow, S. Choo, D. Yao, H. Persson, J. Wei, P. Li, B. Heidecker, W. Ma, R. Varma, L. S. Zhao, D. Perillat, G. Carricato, M. Recknor, K. Du, H. Ho, T. Ellis, J. Gamez, M. Howes, J. Phi-Wilson, S. Lockard, R. Zuk, H. Tan, *Comb. Chem. High Throughput Screening* **2009**, *12*, 791–800.
[28] S. Kumaraswamy, R. Tobias, *Methods Mol. Biol.* **2015**, *1278*, 165–182.
[29] S. Gao, X. Zheng, B. Hu, M. Sun, J. Wu, B. Jiao, L. Wang, *Biosens. Bioelectron.* **2017**, *89*, 952–958.

[30] L. P. Encell, R. Friedman Ohana, K. Zimmerman, P. Otto, G. Vidugiris, M. G. Wood, G. V. Los, M. G. McDougall, C. Zimprich, N. Karassina, R. D. Learish, R. Hurst, J. Hartnett, S. Wheeler, P. Stecha, J. English, K. Zhao, J. Mendez, H. A. Benink, N. Murphy, K. V. Wood, *Curr. Chem. Genomics.* **2012**, *6*, 55–71.
[31] M. Jinek, K. Chylinski, I. Fonfara, M. Hauer, J. A. Doudna, E. Charpentier, *Science* **2012**, *337*, 816–821.
[32] P. Estep, F. Reid, C. Nauman, Y. Liu, T. Sun, J. Sun, Y. Xu, *mAbs.* **2013**, *5*, 270–278.
[33] A. Lin, *FEBS Lett.* **1991**, *287*, 121–124.
[34] P. Novak, G. H. Kruppa, *Eur. J. Mass Spectrom.* **2008**, *14*, 355–365.
[35] Y. Han, Q. Shi, J. Hu, Q. Du, X. Chen, X. Jing, *Macromol. Biosci.* **2008**, *8*, 638–644.
[36] Y. Wang, L. Yan, S. He, D. Zhou, Y. Cheng, X. Chen, X. Jing, Y. Huang, *Macromol. Biosci.* **2018**, *18*, 1700282.
[37] L. Leder, *Methods Mol. Biol.* **2015**,*1266*, 7–27.
[38] W. Yang, L. Restrepo-Pérez, M. Bengtson, S. J. Heerema, A. Birnie, J. van der Torre, C. Dekker, *Nano Lett.* **2018**, *18*, 6469–6474.
[39] P. D. Hsu, D. A. Scott, J. A. Weinstein, F. A. Ran, S. Konermann, V. Agarwala, Y. Li, E. J. Fine, X. Wu, O. Shalem, T. J. Cradick, L. A. Marraffini, G. Bao, F. Zhang, *Nat. Biotechnol.* **2013**, *31*, 827–832.
[40] I. M. Slaymaker, L. Gao, B. Zetsche, D. A. Scott, W. X. Yan, F. Zhang, *Science* **2016**, *351*, 84–88.
[41] W. Deng, X. Shi, R. Tjian, T. Lionnet, R. H. Singer, *Proc. Natl. Acad. Sci. USA* **2015**, *112*, 11870–11875.
[42] S. H. Sternberg, S. Redding, M. Jinek, E. C. Greene, J. A. Doudna, *Nature* **2014**, *507*, 62–67.
[43] L. Uzun, A. Denizli, *Macromol. Biosci.* **2006**, *17*, 791–806.
[44] G. Fabregat, A. Giménez, A. Díaz, J. Puiggalí, C. Alemán, *Macromol. Biosci.* **2018**, *18*, e1800014.
[45] M. Arvand, N. Chaibakhsh, S. Daneshvar, *Food Anal. Methods.* **2015**, *8*, 1911–1922.
[46] Y. L. Jung, C. Jung, J. H. Park, M. I. Kim, H. G. Park, *Chem. Commun.* **2013**, *49*, 2350–2352.
[47] J. J. Storhoff, S. S. Marla, P. Bao, S. Hagenow, H. Mehta, A. Lucas, V. Garimella, T. Patno, W. Buckingham, W. Cork, U. R. Müller, *Biosens. Bioelectron.* **2004**, *19*, 875–883.
[48] K. Ren, Y. Xu, Y. Liu, M. Yang, H. Ju, *ACS Nano* **2018**, *12*, 263–271.
[49] C. Wu, S. Cansiz, L. Zhang, I. T. Teng, L. Qiu, J. Li, Y. Liu, C. Zhou, R. Hu, T. Zhang, C. Cui, L. Cui, W. Tan, *J. Am. Chem. Soc.* **2015**, *137*, 4900–4903.
[50] X. Jiang, H. Wang, Y. Chai, H. Li, W. Shi, R. Yuan, *Anal. Chem.* **2019**, *91*, 10258–10265.
[51] M. L. Ermini, S. Mariani, S. Scarano, M. Minunni, *Biosens. Bioelectron.* **2013**, *40*, 193–199.
[52] J. J. Storhof, A. D. Lucas, V. Garimella, Y. P. Bao, U. R. Müller, *Nat. Biotechnol.* **2004**, *22*, 883–887.

Manuscript received: February 3, 2021
Revised manuscript received: February 26, 2021
Accepted manuscript online: March 8, 2021
Version of record online: ■■, ■■■

FULL PAPERS

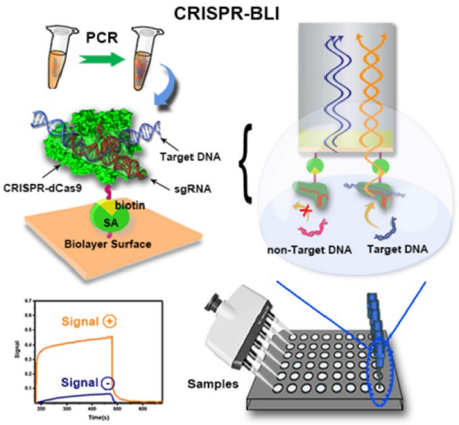

Threefold detection: A CRISPR biosensor is immobilized on a biolayer to construct a CRISPR-BLI platform for DNA detection. The CRISPR-BLI chip is rapid, label-free, and real-time, and has high sequence affinity and specificity due to the properties of BLI and the CRISPR probe. Coupling with PCR improves the sensitivity to 1.34 pg, revealing promising applications in dsDNA detection.